Closed-Form Solution for Timing Analysis of Process Variations on SWCNT Interconnect*

Peng Sun
Dept. of Electronic Engineering
Tsinghua University
Beijing,100084, P. R. China
sun-02@mails.tsinghua.edu.cn

Rong Luo†
Dept. of Electronic Engineering
Tsinghua University
Beijing,100084, P. R. China
luorong@mail.tsinghua.edu.cn

ABSTRACT

In this paper, a comprehensive and fast method is presented for the timing analysis of process variations on single-walled carbon nanotube (SWCNT) bundles. Unlike previous works that based on SPICE tools to estimate the delay, this paper proposes a closed-form solution for SWCNT interconnect timing analysis. With the assumption that the process variations are independent random variables, the delay of SWCNT bundles are mapped to a linear function of the variation variables, and efficiently calculated in the form of probability density functions (PDFs). Compared to SPICE-based solutions, this approach not only saves considerable computation time, but also provides a more comprehensive result, for it shows a compound impact of all variations, and covers all of the potential cases with their corresponding probabilities, rather than only one parameter can vary at a time, and only a worst case estimation is considered. The experiment results show that this solution bears little loss while providing the above mentioned advantages. Compared with SPICE-based Monte Carlo simulations, the experiments report the error in mean and standard deviation of delay to be 1.5% and 1.7% respectively.

Categories and Subject Descriptors

J.6 [**Computer Aided Engineering**]: Computer aided design (CAD)

General Terms

Algorithms, Design

Keywords

Carbon nanotube, Interconnect, Closed-Form, Timing analysis, Process variation

*This work was supported in part by the National Natural Science Foundation of China under Grant 60870001, 60506010 and 90707002.

†contact author, Rong Luo is an associate professor with the Electronic Engineering Department, Tsinghua University, Beijing, 100084, China

SLIP'09, July 26 27, 2009, San Francisco, California, USA.

1. INTRODUCTION

With the process in transistor scaling and increased frequencies, copper interconnect increasingly suffers from severe problems like high resistivity and electromigration [1], and alternative technologies are required to expect better performance of the circuit. Single-walled carbon nanotube (SWCNT) is one of the most competitive replacements for on-chip copper interconnect. Due to its covalently bonded structure, carbon nanotube has an outstanding performance in conductivity and current carrying capabilities [2, 3]. In addition, it is extremely resistant to electromigration [4] and has significantly lower resistance than standard copper interconnect [5].

However, previous researches revealed that compared to the copper interconnect, SWCNT may suffer even more from the variation problem due to the complicated and immature manufacturing process [6, 7, 8]. To understand the impact of process variations more accurately and estimate the results more efficiently are becoming main concerns for future development of CNT interconnects.

In traditional researches about copper interconnects, the variational timing analysis have been fully developed [9, 10, 11, 12, 13, 14, 15, 16]. Substantial research has been performed in mainly 2 approaches, one is the normal SPICE-based estimation, and the other is the well-known statistical estimation, represented by closed-form metrics like Elmore[10], D2M[11], Lognormal[12], and some other metrics involved in lookup tables, like Weibull[13] and h-gamma[14]. The reason that statistical estimation attracts much more attentions in solving variational timing analysis than SPICE tools, is that it not only saves considerable computation time, but provides a comprehensive result more closely to the real-state manufacture process. Basically, the advantages of statistical simulation methods, especially those based on closed-form metrics can be summarized as follows:

1) Computational Efficiency: the delay of CNTs can be directly computed by a simple expression of variation parameters. Even for a large scale circuit design, the results could still be conveniently calculated in a second.

2) Compound Impact: unlike previous researches which assumed only one parameter may vary at a time, this model simulates the compound impact of all the variations of physical dimensions, which is more close to the truth in real manufacture process.

3) Probability Density Functions: by introducing the PDFs, our model provides information about all of the potential cases with the corresponding probabilities, rather than only a best or worst case estimation.

Unlike the copper interconnect researches, few works have paid attention to a closed-form solution in CNT timing analysis. Ref. [8] identified the potential sources of variations on SWCNT bundle interconnect, calculated the relative impact of delay and compared the results with the performance of copper wires. However, the SPICE-based simulation only took into account the worst case of the potential impact, and only one source could vary at each time, which is usually not the truth in the real manufacture process, not to mention the relatively long time period of calculation. All of these might bring considerable inconveniences for designers in future design process, and a closed-form calculation to overcome these problems for CNTs is yet to be explored.

In this paper, a closed-form model to calculate the circuit delay of nanotube interconnects is proposed. In reference to [7], there are ten potential sources of variations to be considered in CNT bundles. To simplify the calculation process and illustrate the method more clearly, we choose only six variations which are weighted most in timing concern. These decided sources are assumed to be independent normal random variables. And the resistance, capacitance, inductance of CNTs given from equivalent RLC model [5, 17, 18, 19] are first expanded by Taylor series, and then transformed approximately into linear functions of these random variables. Based on a similar process, the circuit variability-aware moments can also be computed as linear expressions of RLC, and then as expressions of former random variables. Finally, these variability-aware moments are used in known closed-form delay metrics to compute the interconnect delays, in forms of probability density functions (PDFs). The experiment results reveal that, the timing delays incurred by variations in CNTs are presented in concern of all possible cases with corresponding probabilities, while reflecting the compound impact of all variation sources, and saving large amount of computation time. The loss of accuracy is also acceptable, as compared with Hspice Monte Carlo simulations, this approach report the error in mean and standard deviation of delay to be 1.5% and 1.7%, separately.

This paper is organized as follows. In Section II, we present our approach of a novel closed-form metric for the delay estimation of CNT bundles. In Section III, the experiment results are presented and compared with Hspice results. Final conclusion is given in Section IV.

2. TIMING METRICS FOR PROCESS VARIATION

In this section, a process variation aware metric for timing analysis of CNT bundle interconnects is developed. We begin with a brief introduction of moment-based delay metrics before proposing our methodology to extending these metrics to CNTs area.

For standard copper interconnect, substantial works have been performed to develop accurate metrics for timing analysis. Most of the existing timing metrics involved in calculation of moments, as the process shown in Fig.1 [13]. Using the concept of path tracing, the pth order circuit moment at node i (m_p^i) in a RLC tree can be expressed as

$$m_p^i = \sum_k (-R_{ik}C_k m_{p-1}^i - L_{ik}C_k m_{p-2}^i)$$
$$m_0^i = 1 \qquad (1)$$

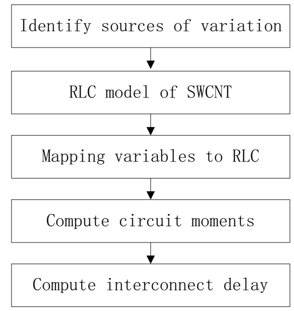

Figure 1: Moment-based-delay-modeling flow

Table 1: Existing delay metrics

Moments	Delay Metrics
One	Elmore, Scaled Elmore
Two	D2M, Weibull
Three	h-gamma, Lognormal

where C_k is the capacitance at node k and $R_{ik}(L_{ik})$ denotes the total overlap resistance(inductance) in the unique paths from the source node to nodes i and k [14].

With the calculation results of circuit moments, the interconnect delay can be efficiently translated using existing metrics in Table I. In our approach, we focus only on closed-form metrics, rather than those requiring lookup tables as our statistical interconnect metrics. Particularly, D2M[11] is selected to illustrate our methodology in this paper. However, this approach is independent of the metric and can be applied to any other closed-form metrics as well.

As summarized below, the steps in our approach will be discussed in details in the following sections:

1) Express RLC parameters of CNT bundles in terms of process variations.

2) Express moments in terms of RLC parameters and hence in terms of process variations.

3) Express interconnect delay as a function of moments and therefore in terms of process variations, with mean and variance of delay distribution as a function of the statistical variables of process variations.

To illustrate our mathematical model in SWCNT timing analysis, six variation candidates are chosen, as shown in Table II, which have the most significant impact to the delay of SWCNT bundles in accordance with the experiment results in paper [7]. The potential dimension sources of variation include (a) the probability that a given nanotube is metallic P_m; (b) inter-bundle nanotube diameter d_t; (c) inter-bundle width w_b; (d) inter-bundle height h_b; (e) inter-bundle variation in the spacing between individual nanotubes s_t; (f) inter-bundle variation in dielectric thickness between interconnect layers h_t. However, this approach is absolutely independent of the number or characters of the sources, which enables designers to configure their lists adaptively with real CNT manufacture cases.

2.1 CNT Interconnect and RLC Model

This section shows the RLC model of SWCNT bundles, which is established following the procedure reported in [5], and the equivalent circuit is shown in Fig.2.

Table 2: Predicted variation in SWCNT bundle process parameters

Variation Type	Geometric Variation
Probability nanotube is metallic(P_m)	$P_m = 1/3$
Inter-bundle nanotube diameter(d_t)	$3\lambda = 23\%$
Inter-bundle width(w_b)	$3\lambda = 32\%$
Inter-bundle height(h_b)	$3\lambda = 32\%$
Inter-bundle nanotube spacing(s_t)	$3\lambda = 23\%$
Inter-bundle dielectric thickness(h_t)	$3\lambda = 32\%$

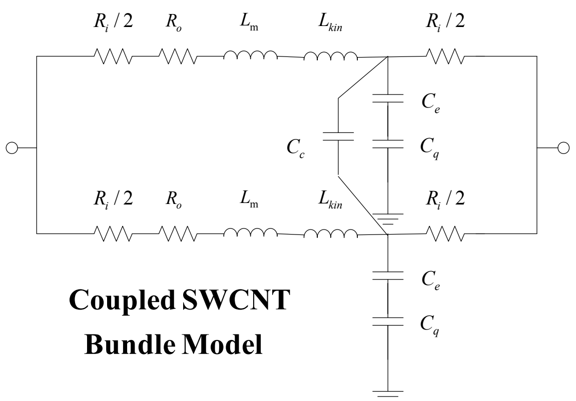

Figure 2: SWCNT bundle interconnect RC model

As illustrated in [5], each SWCNT consists of contact resistance R_c that has fixed value regardless of the interconnect length l_b, and the resistance per unit length R, which depends on both of the bias voltage and the interconnect length .

When the bias voltage $V_b < 0.1V$ [5] , R can be calculated as

$$R = \begin{cases} \dfrac{h}{4e^2} & if \quad l_b < \lambda_t \\ \dfrac{h}{4e^2 C_\lambda d_t} & if \quad l_b > \lambda_t \end{cases} \tag{2}$$

where h is Planck's constant, e is the charge of a single electron, λ_t is the mean-free path, and C_λ is a proportionality constant of λ_t to d_t.

Assuming no current redistribution due to magnetic inductance, the resistance of a bundle of SWCNT is defined by the parallel combination of the individual SWCNT resistances

$$R_b = R_t/n_b \tag{3}$$

here $R_t = R_c + R$, n_b is the number of metallic nanotubes in a given bundle

$$n_b = P_m n_h n_w \tag{4}$$

where P_m is the probability that a nanotube is metallic, n_h and n_w are the number of nanotubes in the vertical and horizontal dimension, respectively.

For SWCNT interconnect, two types of capacitance should be considered, which are the quantum capacitance C_q and the electrostatic capacitance C_e. The quantum capacitance per unit length [20] is given by

$$C_q = \frac{2e^2}{hv_F} \approx 100aF/\mu m \tag{5}$$

where v_F is the Fermi velocity of a carbon nanotube.

As a nanotube has four co-propagating quantum channels, the effective value of the quantum capacitance to be considered in the equivalent circuit is $4C_q$. Since the quantum capacitances of all the CNTs in a bundle appear in parallel, the effective quantum capacitance of the bundle is the sum of the individual quantum capacitances

$$C_q^{bundle} = 4C_q n_b \tag{6}$$

The electrostatic capacitance depends on the bundle geometry and spacing between bundles. According to the analysis of [21], when the bundles are more than fifteen nanotube wide, the variation in capacitance values arising from the variation in nanotube locations is less than 3%. The C_e of the SWCNT bundle can be calculated by representing each bundle as a single conduct of the same width and an equivalent height h_{eq} given by $h_{eq} = h_b(0.5 + 0.3P_m)$.

Thus, the total capacitance of a bundle of SWCNT can be calculated as

$$\frac{1}{C_b} = \frac{1}{C_q^{bundle}} + \frac{1}{C_e^{bundle}} \tag{7}$$

The origination of kinetic inductance L_k is because electrons do not instantaneously respond to the applied electric field. To represent this phenomenon, [22] proposes a model by inserting kinetic inductance given as

$$L_K = \frac{h}{2e^2 v_F} \approx 16nH/\mu m \tag{8}$$

Considering the four co-propagating quantum channels of nanotube, the equivalent value of kinetic inductance is $L_k/4$ [22]. And the kinetic inductance of a SWCNT bundle is thus defined as

$$L_{kb} = \frac{L_k}{4n_b} \tag{9}$$

According to [23], the magnetic inductance primarily depends on the geometry of the bundle and its current return path.

2.2 Mapping Random Variation Variables to RLC Model

Based on the previous RLC model, this section describes our method of simplifying the complicated RLC expressions to linear functions of random variation variables. From equations (1) to (9), we can deduce that R_b, C_b and L_b are all affected by the 6 variation parameters, as they are expressed in polynomial functions of these parameters. Thus, for each polynomial function, we can expand each of the parameters separately through Taylor series. Keeping only the linear terms, the changes in R_b, C_b and L_b due to process variations can be captured by the simple linear approximation shown in equation (10).

$$
\begin{aligned}
R_b &= R_{nom} + a_1 \triangle P_m + a_2 \triangle w_b + a_3 \triangle h_b \\
&\quad + a_4 \triangle d_t + a_5 \triangle s_t \\
C_b &= C_{nom} + b_1 \triangle P_m + b_2 \triangle w_b + b_3 \triangle h_b \\
&\quad + b_4 \triangle d_t + b_5 \triangle s_t + b_6 \triangle h_t \\
L_b &= L_{nom} + c_1 \triangle P_m + c_2 \triangle w_b + c_3 \triangle h_b \\
&\quad + c_4 \triangle d_t + c_5 \triangle s_t + c_6 \triangle h_t
\end{aligned} \tag{10}
$$

where R_{nom}, C_{nom} and L_{nom} are the nominal values of resistance, capacitance and inductance respectively. a_1, b_1 and c_1 represent the change ratio in R_b, C_b and L_b with the change in process variations, and similarly, the other coefficients capture the changes in R_b, C_b and L_b with respect to the corresponding physical dimension. Notice that the variation in dielectric thickness h_t has little effect upon the value of resistance, which means expression of R_b got a monomial less than the expression of C_b and L_b. The coefficients a_i, b_i and c_i can be conveniently computed as

$$
\begin{aligned}
a_1 &= \frac{\partial R_b}{\partial P_m}, a_2 = \frac{\partial R_b}{\partial w_b}, a_3 = \frac{\partial R_b}{\partial h_b} \\
a_4 &= \frac{\partial R_b}{\partial d_t}, a_5 = \frac{\partial R_b}{\partial s_t} \\
b_1 &= \frac{\partial C_b}{\partial P_m}, b_2 = \frac{\partial C_b}{\partial w_b}, b_3 = \frac{\partial C_b}{\partial h_b} \\
b_4 &= \frac{\partial C_b}{\partial d_t}, b_5 = \frac{\partial C_b}{\partial s_t}, b_6 = \frac{\partial C_b}{\partial h_t} \\
c_1 &= \frac{\partial L_b}{\partial P_m}, c_2 = \frac{\partial L_b}{\partial w_b}, c_3 = \frac{\partial L_b}{\partial h_b} \\
c_4 &= \frac{\partial L_b}{\partial d_t}, c_5 = \frac{\partial L_b}{\partial s_t}, c_6 = \frac{\partial L_b}{\partial h_t}
\end{aligned} \tag{11}
$$

As assumed before, changes in the process variations ($\triangle P_m$, $\triangle w_b$, $\triangle h_b$, etc.) are considered as independent normal random variables, thus the resistance, capacitance and inductance calculated in equation (10) are all correlated normal random variables. This is because a linear combination of Gaussian variables also follows a Gaussian distribution. Notice that through this simplification, a bundle of SWCNT can be transformed approximately into a simple RLC model, and the circuit parameters of which can be expressed linearly by variation variables. This implies that a complicated interconnect network built of SWCNT bundles can be expressed as simple RLC model connected together. Fig.3 shows a simple example of such a model of three connected SWCNT bundles.

2.2.1 *Mapping Electrical Parameters to Moments*

Once interconnect dimensions are mapped to the circuit parameters, the next step is to compute the circuit moments. Take the circuit in Fig.3 for example, the first and second order moments of the RLC tree can be obtained as

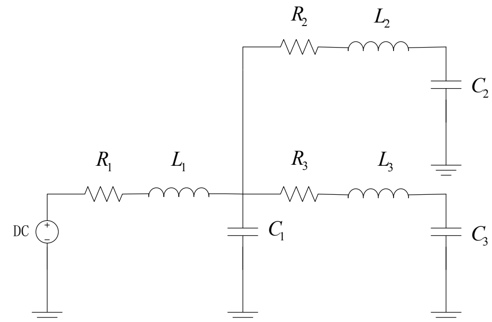

Figure 3: A simple RLC tree

$$
\begin{aligned}
m_1^1 &= -R_1(C_1 + C_2 + C_3) \\
m_1^2 &= -R_1(C_1 + C_2 + C_3) - R_2C_2 \\
m_1^3 &= -R_1(C_1 + C_2 + C_3) - R_3C_3 \\
m_2^1 &= -R_1(C_1m_1^1 + C_2m_1^2 + C_3m_1^3) \\
&\quad - L_1(C_1 + C_2 + C_3) \\
m_2^2 &= -R_1(C_1m_1^1 + C_2m_1^2 + C_3m_1^3) - R_2C_2m_1^2 \\
&\quad - L_1(C_1 + C_2 + C_3) - L_2C_2 \\
m_2^3 &= -R_1(C_1m_1^1 + C_2m_1^2 + C_3m_1^3) - R_3C_3m_1^3 \\
&\quad - L_1(C_1 + C_2 + C_3) - L_3C_3
\end{aligned} \tag{12}
$$

With variations in physical dimensions, R_i, C_i and L_i can be substituted by their corresponding expressions from equation (10) and m_1 can be expressed as

$$
\begin{aligned}
m_1 &= m_{1(nom)} + k_1 \triangle P_m + k_2 \triangle w_b + k_3 \triangle h_b \\
&\quad + k_4 \triangle d_t + k_5 \triangle s_t + k_6 \triangle h_t \\
&\quad + \sum_{X_i \in S, Y_j \in T} k_n(X_iY_j) \\
S &= \{\triangle P_m, \triangle w_b, \triangle h_b, \triangle d_t, \triangle s_t\} \\
T &= \{\triangle P_m, \triangle w_b, \triangle h_b, \triangle d_t, \triangle s_t, \triangle h_t\}
\end{aligned} \tag{13}
$$

here $m_{1(nom)}$ is the nominal value of first moment, which can be calculated from the nominal resistance $R_{i(nom)}$ and capacitance $C_{i(nom)}$ based on equation (12). Suppose the formulation to calculate $m_{1(nom)}$ is expressed as function f

$$
m_{1(nom)} = f(R_{i(nom)}, C_{i(nom)}) \tag{14}
$$

then the parameters k_i in equation (13) can be calculated as

$$
\begin{aligned}
k_1 &= f(a_1^i, C_{nom}^i) + f(R_{nom}^i, b_1^i) \\
k_2 &= f(a_2^i, C_{nom}^i) + f(R_{nom}^i, b_2^i) \\
k_3 &= f(a_3^i, C_{nom}^i) + f(R_{nom}^i, b_3^i) \\
k_4 &= f(a_4^i, C_{nom}^i) + f(R_{nom}^i, b_4^i) \\
k_5 &= f(a_5^i, C_{nom}^i) + f(R_{nom}^i, b_5^i) \\
k_6 &= f(R_{nom}^i, b_6^i)
\end{aligned} \tag{15}
$$

Equation (13) shows that the first moment expression contains higher order terms and cross-product terms, however, the experiment results detailed later show that the higher order terms are not significant and can be neglected without loss of accuracy. Consequently, the first-moment expression can be simplified as a linear function of variations in physical dimensions

$$m_1 = m_{1(nom)} + k_1 \triangle P_m + k_2 \triangle w_b + k_3 \triangle h_b + k_4 \triangle d_t + k_5 \triangle s_t + k_6 \triangle h_t \quad (16)$$

Similarly we can replace the values of m_1 in equation (14), and obtain the following expression of m_2 by keeping only the linear terms

$$m_2 = m_{2(nom)} + A_1 \triangle P_m + A_2 \triangle w_b + A_3 \triangle h_b + A_4 \triangle d_t + A_5 \triangle s_t + A_6 \triangle h_t \quad (17)$$

here $m_{2(nom)}$ is the second moment calculated at nominal resistance $R_{i(nom)}$, nominal capacitance $C_{i(nom)}$ and nominal first moment $m_{1(nom)}$. The formulation of $m_{2(nom)}$ is expressed as function F

$$\begin{aligned} m_{2(nom)} &= F(R_{i(nom)}, C_{i(nom)}, L_{i(nom)}, m_{1(nom)}) \\ &= F_1(R_{i(nom)}, C_{i(nom)}, m_{1(nom)}) \\ &\quad + F_2(L_{i(nom)}, C_{i(nom)}) \end{aligned} \quad (18)$$

then the parameters k_i in equation (13) can be calculated as

$$\begin{aligned} A_j &= F_1(a_j^i, C_{nom}^i, m_{1(nom)}) \\ &\quad + F_1(R_{nom}^i, b_1^i, m_{1(nom)}) \\ &\quad + F_1(R_{i(nom)}, C_{i(nom)}, k_j) \\ &\quad + F_2(c_j^i, C_{nom}^i) + F_2(L_{nom}^i, b_j^i) \end{aligned} \quad (19)$$

2.2.2 Mapping Moments to Delay Metrics

Once the moments are expressed in form of the variation parameters, the PDF of the delay can be correspondingly calculated by mapping that of the moments to the delay metrics. In this paper, D2M is chosen as our delay metric for analysis. However, the approach is independent of the metric and can be applied to any other closed-form metric as well. Thus, the interconnect delay is given by

$$D2M = ln2 \cdot \frac{(m_1)^2}{\sqrt{m_2}} \quad (20)$$

Substituting equations (16) and (17) into (20), expanding the expression using Taylor series expansion and keeping only the linear terms, the D2M expression can be re-written as

$$D2M = ln2 \frac{(m_{1(nom)})^2}{\sqrt{m_{2(nom)}}} (S_1 \triangle P_m + S_2 \triangle w_b + S_3 \triangle h_b + S_4 \triangle d_t + S_5 \triangle S_t + S_6 \triangle h_t) \quad (21)$$

where S_i can be calculated in the form of

$$S_i = \frac{2k_i}{m_{1(nom)}} - \frac{A_i}{2m_{2(nom)}} \quad (22)$$

here $i \in \{1, 2, 3, 4, 5, 6\}$.

As assumed before, $\triangle P_m$, $\triangle w_b$, $\triangle h_b$, $\triangle d_t$, $\triangle s_t$, $\triangle h_t$ are independent random Gaussian variables, and have standard deviations of σ_1, σ_2, σ_3, σ_4, σ_5, σ_6 respectively, the mean and standard deviation of the delay can be formulated as

$$E(D2M) = ln2 \cdot \frac{(m_{1(nom)})^2}{\sqrt{m_{2(nom)}}}$$

$$Stdev(D2M) = ln2 \cdot \frac{(m_{1(nom)})^2}{\sqrt{m_{2(nom)}}} \sqrt{\sum_{i=1}^{6} S_i \cdot \sigma_i} \quad (23)$$

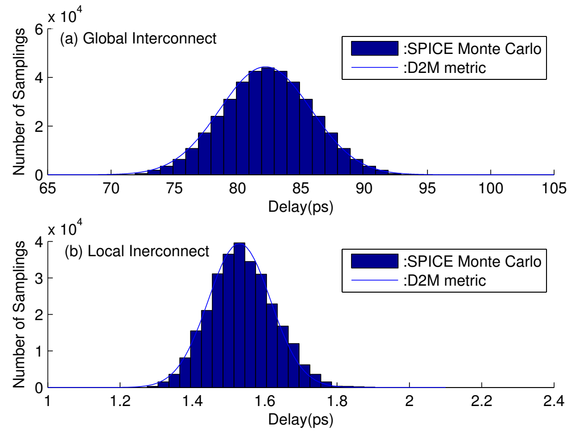

Figure 4: Analytical delay distribution obtained using the statistic D2M metric compared to Monte Carlo simulations for (a) global and (b) local interconnect.

3. EXPERIMENT RESULTS

To calculate the delay using the above mentioned method, a complicated interconnect network based on SWCNT bundles can be simplified into RLC models depicted in Fig.3. Two statistic results based on global and local SWCNT interconnect are provided in Fig.4. and compared with SPICE-based Monte Carlo experiments.

For the global interconnect, the mean and standard deviation of the delay computed using equation (21) matches with the numbers using Monte Carlo simulations. For the local interconnect, there appears a bigger deviation between the two results. This is mainly because in the local interconnects, the impact on delay caused by the variation of d_t tends to be less like a Gaussian one but a lognormal one, and somehow brings some losses of accuracy.

From the test results, one can observe that the proposed method provides a comprehensive result with a compound impact of all variations, while considering all potential cases with the corresponding possibilities. Take the global interconnect for an example, the worst, best and biggest case of the delay are about $94ns$, $71ns$, $82.3ns$,respectively.

When the main concern of the designers is the performance of circuits, a worst case situation may be taken into account. When the designers aim to achieve a balance between performance and resources, the case with the biggest probability may be considered. Considering the error correcting abilities and the balance among the resources, designers can conveniently choose a case which meets the requirements based on their possibilities.

To achieve similar results, the spice-based tools are required to run thousands of times of Monte Carlo simulations, which means large amount of running time consumption and unrealistic for large scale circuits.

However, while meeting the above mentioned advantages, the observations of these results still indicate that the proposed method bears some loss of accuracy. To statistically measure these losses of accuracy, an experiment based on the testbench in paper [24]is provided, as shown in Fig.5. The length of the interconnect line is 1mm, and the interconnect line is divided into 30 identical segments. We performed

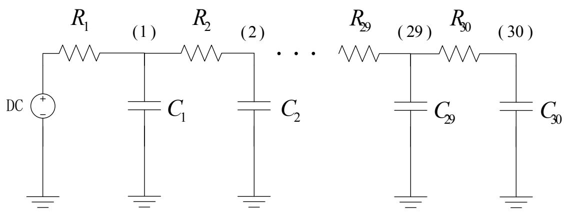

Figure 5: Testbench for Model Verification

Table 3: Delay comparison along various nodes in a simple 30-segment line

Node	Nom(ps)	Mean(ps)		Stdev(ps)	
		Hspice	D2M	Hspice	D2M
15	61.6	61.5	65.1	1.65	1.68
20	82.5	82.2	82.8	2.19	2.15
25	93.7	93.5	93.9	2.51	2.45
30	97.4	97.0	97.4	2.56	2.54
Maximum Error			5.8%	-	1.8%
Average error			1.5%	-	1.7%
Stdev error			0.1%	-	0%

1000 Monte Carlo simulations for each node and compared the mean and standard deviation of Hspice with the results of the proposed model in Table III. The comparison shows that the model works well with almost all the nodes. Although node 15 shows a relatively large error in the mean and variance computation, it is primarily due to the defect of the D2M metric in nominal delay calculation for near-end nodes. Table III also shows the nominal delay computed by using Hspice. We observed here that the mean values of the Monte Carlo simulations are very close to the nominal delays on all the nodes, thereby implying that the Gaussian assumption is applicable for intermediate nodes as well.

4. CONCLUSIONS

We have presented a statistical approach for modeling SWCNT interconnect delay, taking into account the variation effect of physical dimensions. We propose a comprehensive and fast-running solution based on closed-form metrics, and to the best of our knowledge, this is the first statistical timing metric model to analyze the interconnect delay of SWCNT bundles. We take into account six potential sources of variations to derive statistical expressions of the delay of SWCNT interconnects. Experiment results reveal that, our methodology experiences little loss in accuracy compared with HSPICE, with a much shorter computation time and a more comprehensive result. The average error of the statistical D2M model is 1.5% for calculating mean delay time compared to SPICE Monte Carlo simulation, with an average error in standard deviation of only 1.7%.

5. REFERENCES

[1] "International technology roadmap for semiconductors 2007."

[2] P. McEuen, M. Fuhrer, and H. Park, "Single-walled carbon nanotube electronics," *IEEE Transactions on Nanotechnology*, vol. 1, no. 1, pp. 78–85, March 2002.

[3] P. Graham, M. Liebau, G. S. Duesberg, R. Seidel, and E. Unger, "Carbon nanotubes for interconnect applications," *Proc. IEEE Int. Electron Devices Meeting*, pp. 683–686, 2004.

[4] R. H. Baughman, A. A. Zakhidov, and W. A. de Heer,"Carbon nanotubes-the route toward applications," *Science*, vol. 297, pp. 787–792, August 2002.

[5] Y. Massoud and A. Nieuwoudt, "Modeling and design challenges and solutions for carbon nanotube-based interconnect in future high performance integrated circuits," *ACM Journal on Emerging Technologies in Computing Systems*, vol. 2, no. 3, pp. 155–196, July 2006.

[6] M. Liebau, A. P. Graham, G. S. Duesberg, E. Unger, R. Seidel, and F.Kreupl, "Nanoelectronics based on carbon nanotubes: technological challenges and recent developments," *Fullerenes, Nanotubes, and Carbon Nanostructures*, vol. 13, no. 1, pp. 255–258, 2005.

[7] A. Nieuwoudt and Y. Massoud, "Assessing the implications of process variations on future carbon nanotube bundle interconnect solutions," *Proceedings of the 8th International Symposium on Quality Electronic Design*, 2007.

[8] A. Nieuwoudt and Y. Massoud, "On the impact of process variations for carbon nanotube bundles for vlsi interconnect," *IEEE Transaction on Electron Devices*, vol. 54, no. 3, pp. 446–455, 2007.

[9] S. Nassif, "Modeling and analysis of manufacturing variations," *Proceedings of the IEEE Custom Integrated Circuits Conference*, pp. 223–228, May 2001.

[10] W. C. Elmore, "The transient response of damped linear networks with particular regard to wideband amplifiers," *J. Appl. Phys.*, vol. 19, no. 11, pp. 55–63, January 1948.

[11] K. Agarwal, D. Sylvester, and D. Blaauw, "Simple metrics for slew rate of rc circuits based on two circuit moments," *Proc. Design Automation Conf.*, pp. 950–953, 2003.

[12] C. J. Alpert, F. Liu, C. Kashyap, and A. Devgan, "Delay and slew metrics using the lognormal distribution," *Proc. Design Automation Conf.*, pp. 382–385, 2003.

[13] F. Liu, C. Kashyap, and C. J. Alpert, "A delay metric for rc circuits based on the weibull distribution," *Proc. Int. Conf. Computer Aided Design*, pp. 620–624, 2002.

[14] T. Lin, E. Acar, and L. Pileggi, "h-gamma: An rc delay metric based on a gamma distribution approximation to the homogenous response," *Proc. Int. Conf. Computer-Aided Design*, pp. 19–25, 1998.

[15] K. Agarwal, M. Agarwal, D. Sylvester, and D. Blaauw, "Statistical interconnect metrics for physical-design optimization," *Computer-Aided Design of Integrated Circuits and Systems*, vol. 25, no. 7, pp. 1273–1288, 2006.

[16] K. Agarwal, D. Sylvester, and D. Blaauw, "A simple metric for slew rate of rc circuits based on two circuit moments," *IEEE Transactions on Computer-Aided Design of Integrated Circuits and Systems*, vol. 13, no. 9, pp. 1346–1354, 2004.

[17] A. Raychowdhury and K. Roy, "Modeling of metallic carbon-nanotube interconnects for circuit simulations and a comparison with cu interconnects for scaled technologies," *IEEE Transactions on Computer-Aided Design of Integrated Circuits and Systems*, vol. 25, no. 1, pp. 58–65, January 2006.

[18] A. Naeemi, R. Sarvari, and J. Meindl, “Performance comparison between carbon nanotube and copper interconnects for gsi,” *IEEE International Electron Devices Meeting*, pp. 699– 702, December 2004.

[19] D. Rossi, J. Cazeaux, C. Metra, and F. Lombardi, “Modeling crosstalk effects in cnt bus architectures,” *IEEE Transactions on Nanotechnology*, vol. 6, no. 2, pp. 133–145, 2007.

[20] N. Srivastava and K. Banerjee, “Performance analysis of carbon nanotube interconnects for vlsi applications,” *Proceedings of the 2005 IEEE/ACM International Conference on Computer-Aided Design*, pp. 383–390, November 2005.

[21] A. Nieuwoudt and Y. Massoud, “Evaluating the impact of resistance in carbon nanotube bundles for vlsi interconnect using diameter-dependent modeling techniques,” *IEEE Trans. Electron Devices*, vol. 53, pp. 24–60, October 2006.

[22] P. J. Burke, “Luttinger liquid theory as a model of the gigahertz electrical properties of carbon nanotubes,” *IEEE Transactions on Nanotechnology*, vol. 1, no. 3, pp. 129–144, 2002.

[23] A. Nieuwoudt and Y. Massoud, “Carbon nanotube bundle-based low loss integrated inductors,” *7th IEEE Conference on Nanotechnology*, pp. 714–718, August 2007.

[24] L. Saihua, Y. Huazhong, L. Rong, and W. Hui, “Improved statistical interconnect timing analysis considering scattering effect,” *China Academic Journal Electronic Publishing House*, pp. 1918–1922, May 2006.